helix axes, thus contributing a rotation in the opposite sense, *i.e.* laevorotatory. The *RS*1/4 sulphate helix also contributes optical rotation in a laevorotatory sense, but because of the larger sulphate–sulphate distances, to a much lesser extent. The counteracting effect of the NH_4 helix is also small because of the greater NH_4 to NH_4 distances. Models 1 and 2 of Table 4 show that on reducing the polarizability of NH_4^+, the optical rotation is increased, thus showing how they act in an opposite sense with respect to the other helices as far as the optics is concerned. Thus, despite the complexity of this structure, the simple theory seems to work well for the (100) section, which is also the section with the smallest linear birefringence.

It is far more difficult to apply the simple theory to the (010) and (001) sections, as these have large linear birefringences, which dominate over the optical rotation. While it is possible to find some evidence of helical arrangements of polarizable atoms in these sections, it is, therefore, far from clear how they relate to the sense of optical rotation.

AMG is grateful to the Optoelectronics Research Centre at Southampton University for financial support. SA thanks the Gottlieb Daimler- and Karl Benz-Stiftung and the British Council.

References

ANISTRATOV, A. T. & MELNIKOVA, S. V. (1975). *Izv. Akad. Nauk SSSR, Ser. Fiz.* **26**(4), 808–812.
CORAZZA, E. & SABELLI, C. (1967). *Acta Cryst.* **22**, 683–687.
DEVARAJAN, V. & GLAZER, A. M. (1986). *Acta Cryst.* A**42**, 560–569.
FLACK, H. (1983). *Acta Cryst.* A**39**, 876–881.
GLAZER, A. M. & STADNICKA, K. (1986). *J. Appl. Cryst.* **19**, 108–122.
GLAZER, A. M. & STADNICKA, K. (1989). *Acta Cryst.* A**45**, 234–238.
KOBAYASHI, J. & UESU, Y. (1983). *J. Appl. Cryst.* **16**, 204–211.
MOXON, J. R. L. & RENSHAW, A. R. (1990). *J. Phys. Condens. Matter*, **2**, 6807–6836.
NYE, J. F. (1972). *Physical Properties of Crystals.* Oxford: Clarendon Press.
ORTEGA, J., ETXEBARRIA, J. & BRECZEWSKI, T. (1993). *J. Appl. Cryst.* **26**, 549–554.
STADNICKA, K., GLAZER, A. M. & MOXON, J. R. L. (1985). *J. Appl. Cryst.* **18**, 237–240.
STADNICKA, K., MADEJ, A., TEBBUTT, I. J. & GLAZER, A. M. (1992). *Acta Cryst.* B**48**, 16–21.
STOE & CIE (1988). *REDU*4. *Data Reduction Program.* Version 6.2. Stoe & Cie, Darmstadt, Germany.
TESSMAN, J. R., KAHN, A. H. & SHOCKLEY, W. (1953). *Phys. Rev.* **92**(4), 891–895.
THOMAS, P. A. (1987). PhD Thesis, Oxford University.
WATKIN, D. J., CARRUTHERS, J. R. & BATTERIDGE, P. W. (1985). *CRYSTALS User Guide.* Chemical Crystallography Laboratory, Univ. of Oxford, England.

Acta Cryst. (1994). B**50**, 431–435

Structure of the Hofmann Clathrates $Ni(NH_3)_2Ni(CN)_4.2C_6D_6$ and $Zn(NH_3)_2Ni(CN)_4.2C_6H_6$

BY H. G. BÜTTNER AND G. J. KEARLEY

*Institut Laue Langevin, BP*156, 38042 *Grenoble, CEDEX* 09, *France*

C. J. HOWARD

Australian Nuclear Science and Technology Organisation, Lucas Heights Research Laboratories, Private Mail Bag 1, *Menai, New South Wales* 2234, *Australia*

AND F. FILLAUX

Laboratoire de Spectrochimie Infrarouge et Raman, Centre National de la Recherche Scientifique, 2 *rue Henry-Dunant*, 94320 *Thiais, France*

(*Received* 4 *June* 1993; *accepted* 23 *December* 1993)

Abstract

Rietveld analyses of the neutron powder diffraction patterns of $Ni(NH_3)_2Ni(CN)_4.2C_6D_6$ and $Zn(NH_3)_2Ni(CN)_4.2C_6H_6$ have been performed. The space group $P4/m$ is confirmed for $Ni(NH_3)_2Ni(CN)_4.2C_6D_6$ with $a = 7.2196$, $c = 8.1007$ Å at 25 K, $a = 7.2358$, $c = 8.3104$ Å at 300 K. The same space group is found for $Zn(NH_3)_2Ni(CN)_4.2C_6H_6$ with $a = 7.3294$, $c = 8.0722$ Å at 25 K. The effects of

quantum free-rotation of the NH_3 groups is seen clearly in the temperature factors of the ammine protons.

1. Introduction

The Hofmann clathrates (Hofmann & Hocchtlen, 1903) have the general formula $M(NH_3)_2$-$M'(CN)_4.2G$, where M is a six-coordinate and M' a four-coordinate divalent metal ion, and G is an aromatic guest molecule. There has been renewed interest in these compounds since it has been reported that in $Ni(NH_3)_2Ni(CN)_4.2C_6D_6$ the NH_3 groups undergo near quantum free-rotation at 1.8 K (Wegener, Bostoen & Coddens, 1990) and several other Hofmann clathrates have since been found to show the same phenomenon. Quantum free-rotors in molecular crystals are extremely rare and it is important that the crystal structure of these salts at low temperature be known as completely as possible to enable reasonable dynamical models to be developed.

Previous structure determinations at room temperature were performed more than 20 years ago (Rayner & Powell, 1952; Sasaki, 1969), using X-ray diffraction, but H-atom positions were not determined. In the present paper we refine the crystal structures of $Ni(NH_3)_2Ni(CN)_4.2C_6D_6$ at 25 and 300 K and $Zn(NH_3)_2Ni(CN)_4.2C_6H_6$ at 25 K. We will refer to these salts as Ni-Ni.C_6D_6 and Zn-Ni.C_6H_6, respectively.

2. Experimental

Samples of Ni-Ni.C_6D_6 and Zn-Ni.C_6H_6 were prepared and purified according to the procedure given by Baur & Schwarzenbach (1960). The polycrystalline samples were placed in standard thin-walled vanadium sample containers, with temperature control being achieved with a standard helium closed-cycle cryostat.

Diffraction patterns were measured on the fixed-wavelength high-resolution powder diffractometer (HRPD) (Howard, Ball, Davis & Elcombe, 1983) at the HIFAR reactor of the Australian Nuclear Science and Technology Organisation, Lucas Heights, Australia. The patterns were recorded using neutrons of wavelength 1.884 Å.*

3. Data analysis

Crystallographic data are collected in Table 1. Rietveld refinements were achieved using the LHPM3 program (Hill & Howard, 1986). The unit-cell, zero-point, overall scale factor, peak-width/asymmetry and preferred orientation parameters were refined simultaneously with the structural and thermal parameters. A slightly preferred orientation was found along the [011] direction. The observed

Table 1. *Crystallographic data and refinement details with e.s.d.'s in parentheses*

Compound	$Ni(NH_3)_2Ni(CN)_4$-$2(C_6D_6)$ at 300 K	$Ni(NH_3)_2Ni(CN)_4$-$2(C_6D_6)$ at 25 K	$Zn(NH_3)_2Ni(CN)_4$-$2(C_6H_6)$ at 25 K
Space group	*P4/m* (No. 83)	*P4/m* (No. 83)	*P4/m* (No. 83)
Lattice parameters:			
$a = b$ (Å)	7.2358 (6)	7.2196 (3)	7.3294 (3)
c (Å)	8.3104 (8)	8.1007 (5)	8.0722 (4)
Neutron wavelength (Å)	1.884	1.884	1.884
2θ range (°)	16–150	16–150	16–150
2θ scan step (°)	0.06	0.05	0.05
No. of reflections	275	267	272
R_{wp} (%)	4.48	4.83	3.78
R_{exp} (%)	3.84	3.49	3.40
R_B (%)	2.0	2.19	1.66

Table 2. *Atomic positions and thermal parameters* (Å^2) *with e.s.d.'s in parentheses*

	x	y	z	U
$Ni(NH_3)_2Ni(CN)_4.2(C_6D_6)$ at 300 K				
Ni(1)	0	0	0	0.0217 (14)
Ni(2)	½	½	0	0.0217 (14)
N(1)	0.2080 (12)	0.2032 (13)	0	0.0217 (14)
N(2)	0	0	0.2493 (17)	0.0217 (14)
C(1)	0.3176 (20)	0.3219 (18)	0	0.0217 (14)
C(2)	0	½	0.3400 (18)	0.0608 (37)
C(3)	0.1431 (16)	0.4302 (17)	0.4200 (12)	0.0748 (49)
D(2)	0	½	0.2094 (16)	0.0619 (38)
D(3)	0.2598 (22)	0.3733 (18)	0.3547 (18)	0.0981 (53)
H(4)	0.1164 (37)	0.0672 (21)	0.3001 (36)	0.1017 (142)
H(5)	0.0672 (21)	0.1164 (37)	0.3001 (36)	0.1017 (142)
H(6)	0	0.1344 (43)	0.3001 (36)	0.1017 (142)
$Ni(NH_3)_2Ni(CN)_4.2(C_6D_6)$ at 25 K				
Ni(1)	0	0	0	0.0032 (9)
Ni(2)	½	½	0	0.0032 (9)
N(1)	0.2063 (8)	0.2037 (8)	0	0.0032 (9)
N(2)	0	0	0.2598 (11)	0.0032 (9)
C(1)	0.3183 (12)	0.3236 (12)	0	0.0032 (9)
C(2)	0	½	0.3296 (10)	0.0125 (18)
C(3)	0.1497 (9)	0.4293 (10)	0.4148 (8)	0.0272 (22)
D(2)	0	½	0.1963 (9)	0.0214 (20)
D(3)	0.2669 (12)	0.3741 (10)	0.3482 (11)	0.0303 (20)
H(4)	0.1176 (21)	0.0679 (12)	0.3166 (23)	0.0324 (66)
H(5)	0.0679 (12)	0.1176 (21)	0.3166 (23)	0.0324 (66)
H(6)	0	0.1357 (24)	0.3166 (23)	0.0324 (66)
$Zn(NH_3)_2Ni(CN)_4.2(C_6H_6)$ at 25 K				
Zn	0	0	0	0.0032 (12)
Ni	½	½	0	0.0032 (12)
N(1)	0.2088 (10)	0.2076 (10)	0	0.0032 (12)
N(2)	0	0	0.2659 (10)	0.0032 (12)
C(1)	0.3220 (14)	0.3237 (14)	0	0.0032 (12)
C(2)	0	½	0.3290 (10)	0.0063 (19)
C(3)	0.1475 (10)	0.4304 (10)	0.4145 (7)	0.0081 (16)
H(2)	0	½	0.1946 (21)	0.0322 (42)
H(3)	0.2634 (23)	0.3758 (18)	0.3473 (19)	0.0272 (39)
H(4)	0.1164 (28)	0.0672 (16)	0.3119 (26)	0.0377 (86)
H(5)	0.0672 (16)	0.1164 (23)	0.3119 (26)	0.0377 (86)
H(6)	0	0.1343 (33)	0.3119 (26)	0.0377 (86)

* A list of neutron powder diffraction data has been deposited with the IUCr (Reference AL0564). Copies may be obtained through The Managing Editor, International Union of Crystallography, 5 Abbey Square, Chester CH1 2HU, England.

and calculated diffraction patterns are illustrated for Ni-Ni.C_6D_6 (25 and 300 K) and Zn-Ni.C_6H_6 (25 K) in Figs. 1(*a–c*), respectively, and the measures-of-fit are collected in Table 1. Atomic positions and isotropic thermal parameters are given in Table 2.

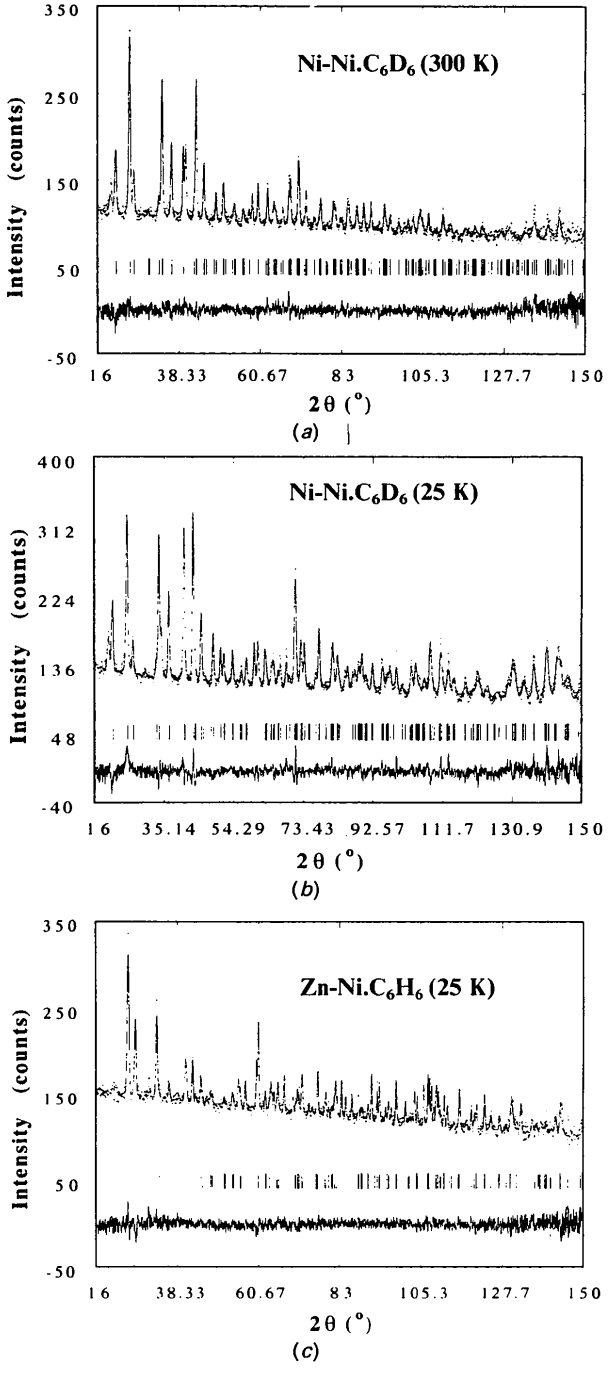

Fig. 1. Observed (crosses), calculated (line) and the difference (lower line) diffraction patterns for $Ni(NH_3)_2Ni(CN)_4.2C_6D_6$ at (*a*) 25, (*b*) 300 and (*c*) $Zn(NH_3)_2Ni(CN)_4.2C_6H_6$ at 25 K. The vertical lines mark the positions of the Bragg reflections.

4. Discussion

4.1. *Description of structure*

The structure of Ni-Ni.C_6D_6 and Zn-Ni.C_6H_6 was found to be consistent with that obtained from earlier X-ray diffraction studies (Rayner & Powell, 1952; Sasaki, 1969). The space group is *P4/m*, with one formula unit in the unit cell. The metal atoms form an infinite-plane network with the cyanide groups forming bridges *via* the N atom to the *M* atom and *via* the C atom to the *M'* atom. An octahedral configuration of the *M* atom is completed by the two axial NH_3 groups. The planes of the benzene rings are perpendicular to the plane of the metal atoms, as shown in Fig. 2.

4.2. *Orientation of benzene molecules*

In the refinements the benzene molecules were constrained to the molecular dimensions reported for solid benzene (David, Ibberson, Jeffrey & Ruble, 1992), with the angle formed between the molecular plane and the *a* axis being a refinable parameter. The refined value of this angle is 64°45′ for both Ni-Ni.C_6D_6 and Zn-Ni.C_6H_6 at 25 K, which is to be compared with the value of 58°30′ reported in a previous study of the Cd-Ni.C_6H_6 analogue.

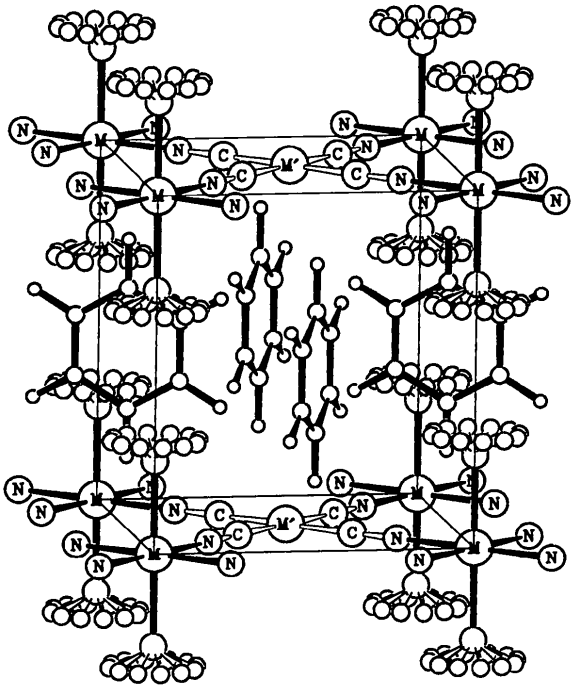

Fig. 2. Illustration of the crystal structure of $M(NH_3)_2$-$M'(CN)_4.2C_6H_6$, showing the disorder of the NH_3 groups and the orientation of the benzene molecules. The thin line denotes the unit cell.

Table 3. *Bond lengths* (Å) *and interbond angles* (°) *with e.s.d.'s in parentheses*

	$Ni(NH_3)_2Ni(CN)_4$·$2(C_6D_6)$ at 300 K	$Ni(NH_3)_2Ni(CN)_4$·$2(C_6D_6)$ at 25 K	$Zn(NH_3)_2Ni(CN)_4$·$2(C_6H_6)$ at 25 K
Ni(1)Zn—N(1)	2.104 (9)	2.093 (6)	2.158 (7)
Ni(1)Zn—N(2)	2.072 (14)	2.105 (9)	2.146 (8)
N(1)—C(1)	1.169 (16)	1.184 (11)	1.188 (13)
C(1)—Ni(2)/Ni	1.844 (14)	1.828 (9)	1.836 (10)
N(2)—H(4)	1.060 (26)	1.082 (15)	1.052 (19)
C(2)—C(3)	1.330 (13)	1.380 (8)	1.380 (8)
C(2)—D(2)/H(2)	1.085 (20)	1.080 (10)	1.085 (19)
C(2)—C(3)—D(3)/H(3)	120	120	120
Ni(1)Zn—N(1)—C(1)	177.05 (0.96)	177.67 (0.61)	179.15 (0.74)
Ni(1)Zn—N(2)—H(4)	113.46 (1.7)	115.11 (1.05)	110.67 (1.2)
Ni(2)Ni—C(1)—N(1)	177.03 (1.19)	177.20 (0.76)	179.04 (0.88)

4.3. *Structural changes between* 25 *and* 300 K

The pattern of Ni-Ni.C_6D_6 at 300 K could not be fitted satisfactorily with the constrained benzene molecule described above. However, when the constraints on bond lengths were removed, whilst retaining the constraint for a planar hexagonal unit, a satisfactory refinement was achieved. The main difference between the benzene molecules in Ni-Ni.C_6D_6 at 25 and 300 K is a foreshortening of the C—C distance, due to thermal motion, from an apparent 1.38 to 1.33 Å, respectively. Bond lengths and angles are given in Table 3.

The length of the *a* axis increased by less than 0.02 Å (0.25%) on warming the sample from 25 to 300 K, whilst the *c* axis increases by more than 0.2 Å (2.5%); this expansion being mainly associated with an increased separation of the NH_3NiNH_3 units. The lack of change in the *a* axis is consistent with the negligible change of angle between the plane of the benzene molecules and this axis over the same temperature range. The slightly longer *a* axis of the Zn analogue is expected as a result of the substitution of a slightly larger metal atom in the metal-atom planes.

4.4. NH_3 *free rotation*

There are four crystallographically equivalent H-atom positions around each ammine N atom. Since the NH_3 groups are known to undergo free rotation even at 25 K, we use the scattering density of an NH_3 group which is rotationally disordered over four equivalent orientations. These orientations were constrained to be related by a rotation of $\pi/6$, as illustrated in Fig. 2, with the radius of rotation and the distance from the N atom to the centre of the H_3 triangle being allowed to refine. Because of the rather approximate treatment of the H-atom thermal parameters, there are large uncertainties in the positional parameters of the ammine H atoms, but nevertheless, the refined radius of rotation, 0.980 Å, compares well with the value of 0.985 Å derived from the rotational spectrum.

4.5. *Thermal parameters*

Because of the presence of H atoms in the NH_3 groups of the Ni-Ni.C_6D_6 sample and in the C_6H_6 group of the Zn-Ni.C_6H_6 sample, the diffraction patterns suffer from substantial background contributions. Consequently, we restricted the number of variables by using a single isotropic temperature factor for both metal atoms, both N atoms and the C atom of the cyanide group. An improved fit was obtained when the atoms of the benzene molecule were allowed individual temperature factors and this resulted in significantly higher temperature factors for the C(3) and H(3) [D(3)] atoms compared with the C(2) and H(2) [D(2)] atoms. This probably reflects some low-frequency whole-body libration of the benzene molecule, even at 25 K.

The use of split-atom positions and isotropic temperature factors is somewhat artificial for the NH_3 free rotors, but nevertheless, the rather large thermal parameters which result from the refinement confirm the presence of free rotation. Further, it was found that when the split-atom model is replaced by a single H atom [H(4)], this scattering centre can be placed anywhere on the circle described by the NH_3 rotations without any effect on the *r*-factors.

We are grateful to ANSTO for providing experimental facilities and financial assistance. We also wish to thank Dr M. F. Lautié from LASIR-CNRS, Thiais, for her skilful preparation of the samples, and Dr A. N. Fitch from ESRF, Grenoble, for helpful discussions.

References

BAUR, R. & SCHWARZENBACH, G. (1960). *Helv. Chim. Acta*, **43**, 842.

DAVID, W. I., IBBERSON, R. M., JEFFREY, G. A. & RUBLE, J. R. (1992). *Phys. Status Solidi B*, **181**, 597–600.

HILL, R. J. & HOWARD, C. J. (1986). *A Computer Program for Rietveld Analysis of Fixed Wavelength X-ray and Neutron Powder Diffraction Patterns*. Australian Atomic Energy Commission (now ANSTO), Report AAEC/M112. Lucas Heights Research Laboratories, New South Wales, Australia.

HOFMANN, K. A. & HOCCHTLEN, F. (1903). *Ber. Dtsch. Chem. Ges.* **36**, 1149.
HOWARD, C. J., BALL, C. J., DAVIS, R. L. & ELCOMBE, M. M. (1983). *Aust. J. Phys.* **36**, 507–518.
RAYNER, J. H. & POWELL, H. M. (1952). *J. Chem. Soc.* pp. 319–328.
SASAKI, Y. (1969). *Bull. Chem. Soc. Jpn*, **42**, 2412.
WEGENER, W., BOSTOEN, C. & CODDENS, G. (1990). *J. Phys. Condens. Matter*, **2**, 3177–3185.

Acta Cryst. (1994). B**50**, 435–441

Synchrotron X-ray Study of the Electron Density in α-Fe_2O_3

BY E. N. MASLEN, V. A. STRELTSOV* AND N. R. STRELTSOVA

Crystallography Centre, University of Western Australia, Nedlands 6009, *Australia*

AND N. ISHIZAWA

Research Laboratory of Engineering Materials, Tokyo Institute of Technology, 4259 *Nagatsuta, Midori-Ku, Yokohama* 227, *Japan*

(*Received* 16 *November* 1993; *accepted* 23 *February* 1994)

Abstract

Structure factors for synthetic haematite, α-Fe_2O_3, have been measured for two small crystals using focused $\lambda = 0.7$ Å synchrotron radiation. The structure factors from the two data sets are consistent. Approximate symmetry in the concordant densities, related more closely to the Fe—Fe geometry than to the nearest-neighbour Fe—O interactions, is similar to that in the corundum α-Al_2O_3 structure. Deformation density maxima are located at the midpoint of the Fe—Fe vector along the c axis, on a common face for O-octahedra, perpendicular to c. Maxima also occur at the midpoint of the Fe–Fe vector bisecting the edges of the O-octahedra. These results are in accordance with theoretical predictions for metal–metal bonding. Space group $R\bar{3}c$, hexagonal, $M_r = 159.7$, $a = 5.0355$ (5), $c = 13.7471$ (7) Å, $V = 301.88$ (7) Å^3, $Z = 6$, $D_x = 5.270$ Mg m^{-3}, $\mu_{0.7} = 13.68$ mm^{-1}, $F(000) = 456$, $T = 293$ K, $R = 0.019$, $wR = 0.021$, $S = 5.55$ for 368 unique reflections in the most accurate data set 2.

Introduction

The deformation density ($\Delta\rho$) near the Al cations for α-Al_2O_3, observed by Maslen, Streltsov, Streltsova, Ishizawa & Satow (1993), has approximate sixfold symmetry. That unexpected topography may be significant to our basic understanding of bonding in solids. It should, therefore, be tested by imaging the electron densities in related compounds. The c/a ratios for most corundum oxide structures, including α-Al_2O_3, α-Fe_2O_3, Cr_2O_3, Ga_2O_3 and Rh_2O_3, range from 2.70 to 2.74 (Prewitt, Shannon, Rogers & Sleight, 1969). That ratio is anomalously small, 2.6388 (3), for Ti_2O_3 (Vincent, Yvon, Grüttner & Ashkenazi, 1980) and anomalously large, 2.8280 (3), for V_2O_3 (Vincent, Yvon & Ashkenazi, 1980). The corundum-type α-Fe_2O_3 unit cell is bigger than that for α-Al_2O_3, but the axial ratio c/a, determined to be 2.731 (1) for crystal (1) and 2.7300 (4) for crystal (2), is within 1 e.s.d. of $c/a = 2.7308$ (3) for α-Al_2O_3.

According to a schematic band structure proposed by Goodenough (1971) for corundum-type 3*d* crystals, the trigonally distorted octahedral crystal field quantized along the threefold axis splits the fivefold-degenerate 3*d* state into a stable σ-bonding pair of e_g orbitals directed toward the nearest-neighbour O atoms, a pair of e_t orbitals directed approximately towards three neighbouring cations in a puckered basal plane through common octahedral site edges, and an a_t orbital directed along the c axis towards one near-neighbour through a common octahedral site face. From symmetry considerations alone, the energy band scheme shows that the bonding a_t and e_t band overlap depends on the c/a ratio and on the widths of these bands.

In theory, the a_t and e_t orbitals for α-Fe_2O_3 are both half filled. Any variation in the c/a ratio that stabilized one would be at the expense of the other. The small c/a ratio of Ti_2O_3 stabilizes a filled and bonding a_t band at the expense of empty e_t bands. The large c/a ratio of V_2O_3 stabilizes the two bonding e_t orbitals per cation relative to the lower a_t band. Experimentally determined $\Delta\rho$ maps for Ti_2O_3 (Vincent, Yvon, Grüttner & Ashkenazi, 1980) and for V_2O_3 (Vincent, Yvon & Ashkenazi, 1980) support

* Author to whom correspondence should be addressed.